

1 Wintertime storage of water in buried supraglacial lakes 2 across the Greenland Ice Sheet

3
4 **L.S. Koenig^{1,2*}, D.J. Lampkin³, L.N. Montgomery³, S.L. Hamilton⁴, C.A. Joseph³,**
5 **S.E. Moutsafa⁵, B. Panzer⁶, K.A. Casey^{7,1}, J.D. Paden⁶, C. Leuschen⁶ and P.**
6 **Gogineni⁶**

7 [1]{Cryospheric Sciences Laboratory, NASA Goddard Space Flight Center, Greenbelt, MD}

8 [2]{now at National Snow and Ice Data Center, University of Colorado, Boulder, CO}

9 [3]{Department of Atmospheric and Oceanic Sciences, University of Maryland, College Park,
10 MD}

11 [4]{Bowdin College, Brunswick, ME}

12 [5]{Department of Geography, Rutgers, The State University of New Jersey, Piscataway, NJ}

13 [6]{Center for Remote Sensing of Ice Sheets, University of Kansas, Lawrence, KS}

14 [7]{Earth System Science Interdisciplinary Center, University of Maryland, College Park,
15 MD}

16 Correspondence to: L.S. Koenig (lora.koenig@colorado.edu)

18 **Abstract**

19 Increased surface melt over the Greenland Ice Sheet (GrIS) is now estimated to account for
20 half or more of the ice sheet's total mass loss. Here, we show that some meltwater is stored,
21 over winter, in buried supraglacial lakes. We use airborne radar from Operation IceBridge
22 between 2009 and 2012 to detect buried supraglacial lakes, and find that they were distributed
23 extensively around the GrIS margin through that period. Buried supraglacial lakes can persist
24 through multiple winters and are, on average, $\sim 1.9 + 0.2$ m below the surface. Most buried
25 supraglacial lakes exist with no surface expression of their occurrence in visible imagery.
26 The few buried supraglacial lakes that do exhibit surface expression have a unique visible
27 signature associated with a darker blue color where subsurface water is located. The volume
28 of retained water in the buried supraglacial lakes is likely insignificant compared to the total

1 mass loss from the GrIS, but the water may have important implications locally for the
2 development of the englacial hydrologic system and ice temperatures. Buried supraglacial
3 lakes represent a small but year-round source of meltwater in the GrIS hydrologic system.

4 **1 Introduction**

5 Annual mass loss from the Greenland Ice Sheet (GrIS) has increased substantially,
6 quadrupling in the last two decades (Shepherd et al., 2012). Warming Arctic temperatures
7 (e.g. Comiso, 2003; Hall et al., 2013) and a decrease in ice-sheet albedo (e.g. Angelen et al.,
8 2014; Box et al., 2012; Tedesco et al., 2011) have increased surface melt which now accounts
9 for half or more of the total mass loss, outpacing ice dynamics in recent years (van den
10 Broeke et al., 2009; Enderlin et al., 2014; Khan et al., 2014). Even with the increasing GrIS
11 surface melt, highlighted by a record melt and runoff event in 2012 (Nghiem et al., 2012; Hall
12 et al., 2013; Hanna et al., 2014), the meltwater mass fluxing through and retained within the
13 supra-, en- and subglacial hydrologic networks is relatively unquantified making ice-sheet
14 wide water budgets difficult to balance (Rennermalm et al., 2013; Forster et al., 2013).

15 While regional climate models agree relatively well on precipitation amounts across the GrIS
16 (~20% variance), they still have large discrepancies in melt production, refreezing, and runoff
17 (from 38-83% variance, Vernon et al., 2013). This is due not only to differences in the
18 models, but also insufficient field observations for quantifying meltwater retention, transport
19 and runoff (Rennermalm et al., 2013). Field observations have only recently discovered large
20 amounts of water retention (Forster et al., 2013; Koenig et al., 2014) and latent heating from
21 refreezing (Harper et al., 2012; Humphreys et al., 2012) on the perimeter of the GrIS, and
22 model improvements to account for the water retention are still in their initial stages (Kuipers
23 Munneke et al., 2014). These recent discoveries punctuate that more observations are needed
24 of the GrIS hydrologic system, especially at and just below the ice-sheet surface, to fully
25 understand meltwater transport and eventual runoff.

26 This paper presents an initial study and mapping of over-winter surface-melt retention in
27 buried supraglacial lakes (Figure 1) within the GrIS. We define a “buried supraglacial lake,”
28 hereafter for brevity a “buried lake,” as water retained through a winter season at shallow
29 depths within the ice sheet that originally formed, during a previous melt season, as a
30 (subaerial) supraglacial lake. Thus, a buried lake is a specific type of supraglacial lake that
31 spans the boundary between the supra- and englacial hydrologic system, exists under lake ice

1 and snow/firn layers in some seasons, and can re-emerge as a supraglacial lake in others.
2 Near-surface, high-resolution radar data, collected during the Arctic spring campaigns of
3 Operation IceBridge (OIB), clearly show water retention in buried lakes through the winter
4 season. In this paper, we use OIB radar data to map the extent and depth of buried lakes
5 across the GrIS. This effort is the first to characterize wintertime meltwater storage in buried
6 lakes over the GrIS and provide an assessment of its impact on the hydrologic system.

7 **2 Background**

8 Several researchers have studied supraglacial lakes that are easily distinguishable by visible
9 and radar satellites when they form seasonally in the ablation and percolation zones across the
10 GrIS (Echelmeyer et al., 1991; Box and Ski, 2007; McMillan et al., 2007; Sneed and
11 Hamilton, 2007; Sundal et al., 2009; Lampkin, 2011; Selmes et al., 2011; Tedesco and Steiner,
12 2011; Howat et al., 2013). Supraglacial lakes form in local topographic lows formed by
13 bedrock depressions, which are not advected by the ice, and often reform in the same
14 locations (Echelmeyer et al., 1991; Box and Ski, 2007; Selmes et al., 2011). Das et al., (2008)
15 observed the rapid (< 2 hours) drainage of a supraglacial lake through fractures, delivering
16 surface meltwater to the bedrock-ice interface causing local uplift and glacier acceleration.
17 Further studies have expanded the links between supraglacial lakes, and water-filled
18 crevasses, to the en- and subglacial hydrologic system, clearly showing that surface meltwater
19 can be routed to the bed of the GrIS affecting ice dynamics. (Zwally et al., 2002; Joughin et
20 al., 2008; Catania et al., 2008; Bartholomew et al., 2011; Palmer et al., 2011; Sundal et al.,
21 2011; Hoffman et al., 2011; Tedstone et al., 2013).

22 Most studies assume that supraglacial lakes either drain during the summer, through the
23 supraglacial or englacial hydrologic system, or refreeze during the winter. Few studies have
24 investigated the behavior of supraglacial lakes during the winter season. Ohmura et al. (1991)
25 attributed the presence of ice plates they observed on the snow surface at West Lake near
26 Swiss Camp, Western Greenland, to the persistence of water late into winter, which formed a
27 frozen ice layer and then drained. Additionally, they detected a deep lake (~10 m) to the east
28 of Swiss Camp that likely remained water-filled through the winter, and developed lake ice up
29 to 1.5 m thick, before it drained in spring or early summer. Rennermalm et al. (2013) also
30 reported evidence of water retention somewhere within the GrIS hydrologic system, from
31 peaks in stream discharge that occur in the fall and spring, up to 6 months after surface melt.

1 The buried lakes that we identify and map, using radar data, in this paper represent a hitherto
2 understudied proportion of wintertime storage of water.

3

4 **3 Data**

5 **3.1 Radar data**

6 To identify and map subsurface water we use data acquired by the CReSIS ultra-wideband
7 Snow Radar during OIB Arctic Campaigns from 2009 through 2012 (Leuschen, 2014). The
8 radar operates over the frequency range from ~2 to 6.5 GHz where water has a high
9 absorption coefficient resulting in the attenuation of radar waves and a strong reflection of the
10 wave at the ice-water interface due to the large difference between the dielectric constant of
11 ice and water (Figure 2) (Ulaby et al., 1981). The Snow Radar uses a Frequency Modulated
12 Continuous Wave (FMCW) design which provides a vertical resolution of ~4 cm in snow/firn
13 to a depth of tens of meters. Radar backscatter along a transect is often displayed as an
14 echogram (Figure 2) which provides a visual image of the subsurface returns. For additional
15 details on the Snow Radar performance see Panzer et al. (2013) and Rodriguez-Morales et al.
16 (2014).

17 **3.2 Visible and thermal imagery**

18 Visible imagery from several imaging platforms is used to support the analysis of buried
19 lakes. OIB Digital Mapping System (DMS) imagery, acquired coincident with Snow Radar
20 data, is used to examine surface features indicative of the presence of subsurface water.
21 Cloud-free Moderate Resolution Imaging Spectroradiometer (MODIS) Rapid Response
22 Arctic Subset true color imagery (250 m resolution) is used to determine whether (subaerial)
23 supraglacial lakes formed previously at the locations of the radar-located buried lakes.
24 Additionally, at a sample lake site, MODIS Land Surface Temperature (LST) data are used to
25 corroborate melt onset and surface thermal conditions and Landsat Enhanced Thematic
26 Mapper (ETM+) panchromatic imagery, with a resolution of ~15 m, is used to evaluate the
27 summertime evolution of the lake.

28 DMS acquires imagery in the visible part of the electromagnetic spectrum at a nominal
29 resolution of 10 cm (at 1500 feet AGL, the nominal OIB flight altitude). DMS collects data
30 over three multispectral and panchromatic bands using a 21 megapixel Canon EOS 5D Mark

1 II digital camera. Data are orthorectified and corrected for camera orientation using the
2 Applanix POS/AV navigation system. For additional details see Dominguez (2014).

3 MODIS LST (MOD11A1, version 5.1) swath data at 1 km resolution are accurate to within \pm
4 1°C (Wan et al., 2002) for snow and ice surface temperatures between -15 to 0°C (Hall et al.,
5 2008). MODIS LSTs acquired over the GrIS, however, can be ~ 1 to 3 degrees colder than
6 the actual surface temperatures (Hall et al. 2013; Koenig and Hall, 2010).

7 **4 Methods**

8 **4.1 Detection of buried lakes from airborne radar**

9 All Snow Radar echograms over the GrIS from 2009-2012 (e.g. Figure 2B) were inspected
10 manually for subsurface attenuations of the radar backscatter, which could be attributed to a
11 buried lake. To ensure the radar response was associated with englacial water, and not some
12 other density or dielectric change, all 2011 detections from Snow Radar data were compared
13 to either the Accumulation Radar (~ 600 - 900 MHz) or MCoRDS Radar (~ 140 - 260 MHz),
14 flown simultaneously with the Snow Radar onboard the OIB aircraft (Figure 2). Water
15 attenuates across radar frequencies. If at least one additional radar showed attenuated
16 backscatter the detection remained in the dataset. Additionally, all detections were compared
17 to summertime cloud-free MODIS imagery to evaluate whether a subaerial supraglacial lake
18 formed at a given radar-located buried lake's location during a preceding melt season (Figure
19 3). The 2011 Snow Radar data were chosen for this initial analysis because it was the first
20 year in which the OIB radar operators discovered the unique return over supraglacial lake
21 regions.

22 The analysis of the 2011 Snow Radar data led to two characteristic echogram patterns for
23 englacial water retention: buried lakes (e.g. Figure 2B) and water-filled crevasse fields. The
24 water-filled crevasse fields were not included in the analysis presented here because, though it
25 is likely they contain englacial water, it is also possible that the crevasses themselves, or hoar
26 crystals formed within them, scatter the radar signal in a manner that cannot be distinguished
27 from scatter caused directly by reflections off subsurface water. Additional field verification,
28 beyond the scope of this study, would be needed to interpret radar backscatter over crevassed
29 regions.

30 The detected buried lake from 2011 were mapped using approximately each lake's center
31 point, and were compared to high resolution (cm-scale) DMS imagery of the GrIS surface

1 coincident with the radar collection (Figure 4) (Dominguez, 2014). DMS imagery was used
2 to characterize visually the surface roughness, detect crevasses and look for any distinct
3 surface expression of the buried lakes.

4 Finally, to construct time series of buried lakes, the characteristic buried-lake radar returns
5 (Figure 2B), determined as we have outlined from the 2011 data, was used to map buried
6 lakes in OIB Snow Radar data from the 2009, 2010 and 2012. Buried lakes that formed
7 within 1 km of each other from year-to-year were considered the same feature. This is
8 justified considering Selmes et al. (2011), who reported a median area of 0.56 km² and a
9 mean area of 0.80 km² for lakes across the GrIS. Because the buried lakes are mapped using
10 an approximate center point, a 1 km radius is a reasonable distance to be considered the same
11 feature along the changing OIB flight lines.

12 **4.2 Depth retrieval of the water surface**

13 The 2009-2012 Snow Radar echograms of the buried lakes were digitized manually to
14 determine the depth from the snow surface to the water surface. If distinguishable in the
15 echogram, as shown in Figure 2B, both the snow/lake-ice interface and the lake-ice/water
16 interface were digitized. When a snow layer was digitized, a reasonable near-surface snow
17 density of 320 kg/m³ (Benson, 1962), was assumed to convert radar travel time to depth using
18 equations developed by Wiesmann and Matzler (1999). When a lake ice layer was digitized
19 or if only the snow surface and the water layer were digitized, the dielectric properties of ice
20 were assumed to convert radar travel time to depth (relative permittivity, $\epsilon' = 3.2$, Dowdeswell
21 and Evans, 2004). In the absence of field data providing a stratigraphic density profile, the
22 adoption of ice density values biases the depth measurements to shallower depths.
23 Uncertainties in the depth were estimated by taking the subset of radar echograms where a
24 snow layer was detected and calculating the depth with both the snow layer and ice
25 assumptions. The average percent difference defines the uncertainty at 9% (range of 2% to
26 24%) shallow.

27 **5 Results**

28 **5.1 Spatial and temporal distribution of buried lakes**

29 The wintertime storage of meltwater in buried lakes is extensive around the margin of the
30 GrIS (Figure 5). All buried lakes identified from 2009-2012 were below the 2000 m contour

1 with the majority detected between 1000 m and 2000 m on the west coast of the ice sheet
2 (Figure 5). Table 1 provides the number of buried lakes detected each year, the mean and
3 standard deviation of buried lake elevation, the number of buried lakes below 1000 m and the
4 number of lakes detected per 1000 km of OIB flight lines flown below 2000 m. Because OIB
5 is an airborne mission with a changing set of flight lines leading to an inconsistent spatial
6 sampling, and thus regionally biased sampling, these results must be analysed with caution
7 and in full appreciation of the characteristics of the survey campaigns. Thus, for example,
8 while in Table 1 it appears that more lakes were detected in 2011 there were also more
9 flightlines in 2011 below 2000 m and many of these were along the west coast.

10 Clusters of buried lakes are concentrated along the west coast of Greenland and near 79 N
11 Glacier where OIB gridded flight lines are flown repeatedly in multiple years (Figure 5). It is
12 also in these regions where we detect buried lakes that persist for multiple years (Figure 5).
13 Again, these multi-year detections must be taken in the context that they are detected in areas
14 with high concentrations of supraglacial lakes where OIB flightlines are repeated in multiple
15 years. It is very likely that other buried lakes are present through multiple winters yet were
16 not detected in more than one year due to the limited OIB spatial and repeat sampling. In
17 total, 53 lakes were detected in two of the four years and 7 lakes were detected in three of the
18 four years (Figure 5). All lakes detected over three seasons are located on the OIB grid near
19 Jakobshavn Isbræ that is repeated annually.

20 **5.2 Surface expression of buried lakes and lake evolution**

21 DMS imagery rarely shows any surface expression of buried lakes. Only at five locations was
22 a unique surface expression found when the buried lake's ice covered surface was exposed.
23 Two examples are shown in Figures 4 and 6. These figures show a surface expression of the
24 darker blue ice adjacent to a region of lighter colored ice that corresponds with the transitional
25 zone from water detection (attenuation) to no water detection (penetration) in the radar
26 echograms (Figures 4 and 6). The darker blue color associated with the retained water can be
27 explained by the vibrational transitions as well as the higher density and temperature of water
28 molecules in the buried lake resulting in stronger hydrogen-oxygen bond absorption feature
29 near 600 nm (Grenfell and Perovich, 1981; Warren, 1984). The hydrogen bonds in water
30 cause a shift to lower energy, over that of ice, which can produce the darker blue color (Luck,
31 1980; Langford et al., 2001). Unfortunately the DMS data used here cannot directly quantify
32 the spectral signature.

1 Figure 6 shows a radar echogram and DMS image of a lake detected on May 2, 2011,
2 approximately 100 km inland from the terminus of 79 N Glacier in Northern Greenland.
3 Radar backscatter clearly shows melt on the surface (Figure 6 between locations 3 and 4)
4 likely driven by radiative heating. The rest of the frozen lake (Figure 6 between locations 1
5 and 2) and buried lake (Figure 6 between locations 2 and 3) has persistent accumulated snow
6 insulating the ice underneath and preventing the onset of melt. Landsat ETM+ images during
7 the peak of the 2011 melt season (Figure 7) demonstrate that lake extent corresponds to
8 regions in the radar echogram where melt was initiated (Figure 7 between locations 3 to 4)
9 and that the region of the buried lake (Figure 7 between locations 2 and 3) maintained a
10 floating ice cap into the melt season. MODIS LST data, the only temperature data available
11 for this site and date, show a peak temperature of -10.7 C during the 1640 GMT overpass.
12 The Snow Radar and DMS data were acquired at 1609 GMT when OIB overflowed the site very
13 close to the peak temperature and solar input. The MODIS LST, however, is rather low for
14 the production of water observed in the echogram over this site which is probably the result of
15 the relatively coarse spatial resolution (1 km) of MODIS such that the very small patch of
16 surface melt, or melt from a few cm below the surface, at the edge of the lake, was not
17 resolved. The evolution of this particular buried lake into the melt season is concentrated
18 melting around the perimeter of the lake while the deeper center of the lake remains insulated
19 with a floating cap, likely increasing the probability it will persist throughout the next winter
20 season barring some supra- or englacial drainage event. These data also indicate that the early
21 onset of melt is spatially heterogeneous, primarily occurring at locations where darker ice is
22 exposed, and that some of the first melt of the season is associated with exposed buried lakes.

23 **5.3 Depth distribution of buried lakes**

24 Figure 8 shows a histogram of the digitized water layer depths from every radar return over a
25 buried lake. The average depth to the retained water during the April and May OIB flights
26 from 2009 to 2012 is 1.88 ±0.16 m with a total range of 0.05 ±0.01 m to 9.43 ±0.85 m and a
27 standard deviation of 1.30 m. There is not a distinctive pattern in buried lake depths along the
28 margins of the GrIS. 38% of radar returns delineated a snow layer above the lake ice with an
29 average snow layer thickness over the buried lakes of 0.65 m (range of 0.15 m to 2.93 m) and
30 an average ice layer thickness below the snow of 1.40 m (range of 0.4 m to 4.58 m).
31 Uncertainties associated with estimates of density stratigraphy across the GrIS, which is used

1 to convert radar travel time to depth, likely cause a shallow bias in these depth measurements
2 of on average 9% and up to 24%.

3

4 **6 Discussion**

5 **6.1 Buried lakes and surface mass budget**

6 Though the water stored in buried lakes is spatially extensive, it represents only a very small
7 amount of mass likely of little consequence to mass loss projections for Greenland.
8 Assuming all the buried lakes detected in 2011, the year with the maximum number of lakes,
9 were the size of the mean supraglacial lake detected by Selmes et al. (2011), with a large
10 water depth of 10 m, the volume of water retained in the lakes would amount to ~1.5 Gt of
11 water over an area of ~ 140 km². For comparison it is estimated that the firn aquifer covering
12 ~70,000 km² of southeast Greenland holds ~140 Gt of water (Forster et al., 2013; Koenig et
13 al., 2014) while recent models put GrIS runoff at between 100 and 300 Gt annually (Vernon
14 et al., 2013). The importance of buried lakes does not, therefore, lie so much in mass-loss
15 contributions; rather the spatial distribution of the retained water is locally important for the
16 development of the hydrologic system and ice temperatures.

17 **6.2 Lake evolution and implications for the hydrologic cycle**

18 The buried lakes identified and mapped in this study represent a newly documented class, or
19 subset, of supraglacial lake. We emplace their formation with the following conceptual
20 model. Once formed, a supraglacial lake can 1) drain through the englacial or supraglacial
21 hydrologic system at some time throughout the year, most often during the melt season 2)
22 refreeze completely during the winter season or 3) partially freeze during the winter season,
23 form lake ice, and retain water at depth, becoming a buried lake. Buried lakes can resurface
24 in the following melt season or remain buried for multiple seasons before re-emerging at the
25 surface. As shown in Figure 7, many of the re-emerging lakes have a characteristic crescent
26 or toroid shape and maintain a floating cap of ice into the melt season. The formation of
27 buried lakes on the GrIS follows the natural wintertime evolution of lake-ice formation
28 observed over Arctic lakes on land, with similar ice thicknesses ranging between 1 and 2 m
29 (e.g. Surdu et al., 2014). GrIS buried-lake formation also parallels meltpond refreezing on sea
30 ice, wherein trapped ponds are created and persist until complete refreezing is accomplished
31 (Flocco et al., 2015). Satellite images of the summertime extent of the supraglacial lakes

1 paired with the subsurface radar data shown here suggest that at elevations above 1000 m all
2 three types of supraglacial lakes coexist in the same region, all experiencing the same
3 meteorological forcings. How and which supraglacial lakes become buried lakes, is still
4 unanswered but a discussion of possible formation mechanisms and evolution is warranted.

5 The initial formation of a buried lake is likely dependent on two factors 1) the degree of
6 connectivity of the lake to the supra- and englacial hydrologic system responsible for the
7 transport of water out of the lake and 2) the water volume stored in the lake at the end of the
8 melt season, particularly the depth, which determines the energy balance required to freeze.
9 Without further research and modeling it is unclear if either connectivity or depth is the more
10 predominate factor in predicting buried-lake formation but, with increasing melt extent across
11 the GrIS (Mote et al, 2007; Nghiem et al., 2012; Hall et al., 2013), both may increase over
12 time.

13 When a buried lake reaches the surface, and thaws, it will initially contain a larger amount of
14 water in the lake basin than a neighboring drained basin at the start of the melt season. As the
15 season progresses less meltwater will be needed to fill the already partially-filled basin. A
16 more efficient filling of the lake basin would lead to more efficient overtopping and surface
17 overflow, eventually leading to the development of supraglacial channels. Buried lakes tend
18 to be prevalent at elevations coincident with the occurrence of lakes associated with more
19 than one outflow channel (Lampkin et al., 2013). It is, therefore, possible buried lakes, over
20 time, promote supraglacial channel development leading to a more connected lake basin and
21 diminishing the chances of a buried lake forming in subsequent seasons. More research is
22 needed but if this scenario is true, a buried lake may be a transient process in the development
23 of a more efficient hydrologic system.

24 The retained water in buried lakes will also warm ice locally at the surface of the ice sheet as
25 measured and modeled by Humphreys et al. (2012) and Kuipers Munneke et al. (2014). If
26 the buried-lake water infiltrates cracks at the base of the lake it is capable of delivering
27 meltwater, and its associated latent heating, deeper into the ice sheet. The resultant heating
28 and softening of the ice could affect ice-flow dynamics, especially if concentrations of buried
29 lakes are located at lateral margins of outlet glaciers. The rise in ice temperatures around
30 conduits would also make it easier to activate the conduit in the spring/summer, supporting
31 the hypothesis that buried lakes are part of the evolutionary cycle towards a more efficient
32 drainage system. Considering this mechanism, buried lakes provide a possible water source

1 for the peaks in stream discharge observed by Rennermalm et al. (2013) when no surface melt
2 was present. Buried lakes represent a mechanism to extend surface meltwater infiltration
3 deeper into the GrIS at any time during the year.

4 **7 Conclusions**

5 Buried supraglacial lakes are extensively distributed around the margins of the GrIS. A few
6 previous studies suggested that water remained in the supraglacial lakes late into the winter
7 season; however, these data are the first to confirm and map extensively the distribution of the
8 retained water. Though the water retained in buried supraglacial lakes is insignificant
9 compared to total mass loss, it has important implications for the local temperature profile,
10 development of the englacial hydrologic network and ice dynamics. This research presents a
11 new understanding of meltwater routing through and within the GrIS and emphasizes the need
12 to better understand the hydrologic pathways through which meltwater drains toward the
13 ocean.

14 **Acknowledgements**

15 The authors thank L. Brucker and T. Neumann for their insightful discussions. This work was
16 supported by the NASA's New Investigator and Cryospheric Sciences Programs. Data
17 collection and instrument development were made possible by The University of Kansas'
18 Center for Remote Sensing of Ice Sheets (CReSIS) supported by the National Science
19 Foundation and Operation IceBridge. S.E.M supported by NASA's Earth and Space Science
20 Fellowship Program grant NNX12AN98H.

21

1 **References**

- 2 Angelen, J. H., Broeke, M. R., Wouters, B., & Lenaerts, J.: Contemporary (1960-2012)
3 evolution of the climate and surface mass balance of the Greenland ice sheet. *Surveys in*
4 *Geophysics*, 35(5), 1155-1174. doi:[http://0-dx.doi.org/libraries.colorado.edu/10.1007/s10712-](http://0-dx.doi.org/libraries.colorado.edu/10.1007/s10712-013-9261-z)
5 013-9261-z, 2014.
- 6 Bartholomew, I., Nienow, P., Sole, A., Mair, D., Cowton, T., Palmer, S. and Wadham, J.:
7 Supraglacial forcing of subglacial drainage in the ablation zone of the Greenland ice sheet,
8 *Geophys. Res. Lett.*, 38, doi:10.1029/2011GL047063, 2011.
- 9 Benson, C. S.: Stratigraphic studies in the snow and firn of the Greenland Ice sheet. *SIPRE*
10 *Res. Rep.* 70, 1962.
- 11 Box, J. E. and Ski, K.: Remote sounding of Greenland supraglacial melt lakes: implications
12 for subglacial hydraulics, *J. Glaciol.*, 53(181), 257–265, doi:10.3189/172756507782202883,
13 2007.
- 14 Box, J. E., Fettweis, X., Stroeve, J. C., Tedesco, M., Hall, D. K., & Steffen, K.: Greenland ice
15 sheet albedo feedback: Thermodynamics and atmospheric drivers. *The Cryosphere*, 6(4), 821,
16 2012.
- 17 Van den Broeke, M., Bamber, J., Ettema, J., Rignot, E., Schrama, E., van de Berg, W. J., van
18 Meijgaard, E., Velicogna, I. and Wouters, B.: Partitioning Recent Greenland Mass Loss,
19 *Science*, 326, 984–986, doi:10.1126/science.1178176, 2009.
- 20 Catania, G. A., Neumann, T. A. and Price, S. F.: Characterizing englacial drainage in the
21 ablation zone of the Greenland ice sheet, *J. Glaciol.*, 54(187), 567–578,
22 doi:10.3189/002214308786570854, 2008.
- 23 Comiso, J. C.: Warming Trends in the Arctic from Clear Sky Satellite Observations, *J. Clim.*,
24 16(21), 3498–3510, doi:10.1175/1520-0442, 2003.
- 25 Das, S. B., Joughin, I., Behn, M. D., Howat, I. M., King, M. A., Lizarralde, D. and Bhatia, M.
26 P.: Fracture propagation to the base of the Greenland Ice Sheet during supraglacial lake
27 drainage., *Science*, 320(5877), 778–81, doi:10.1126/science.1153360, 2008.
- 28 Dominguez, R.: IceBridge DMS L1B Geolocated and Orthorectified Images, Boulder,
29 Colorado, NASA DAAC at the National Snow and Ice Data Center, accessed 2014.

1 Dowdeswell, J. A. and Evans, S.: Investigations of the form and flow of ice sheets and
2 glaciers using radio-echo sounding, *Rep. Prog. Phys.*, 67(10), 1821–1861, doi:10.1088/0034-
3 4885/67/10/R03, 2004.

4 Enderlin, E. M., Howat, I. M., Jeong, S., Noh, M. J., van Angelen, J. H. and van den Broeke,
5 M. R.: An improved mass budget for the Greenland ice sheet, *Geophys. Res. Lett.*, 41(3),
6 866–872, doi:10.1002/2013GL059010, 2014.

7 Echelmeyer, K., Clarke, T. S. and Harrison, W. D.: Surficial glaciology of Jakobshavn Isbræ,
8 West Greenland 1. Surface-morphology, *J. Glaciol.*, 37, 368–382, 1991.

9 Flocco, D., Feltham D. L., Bailey, E. and Schroeder, D.: The refreezing of melt ponds on
10 Arctic sea ice, *J. Geophys. Res. Oceans*, 120, doi:10.1002/2014JC010140, 2015.

11 Forster, R. R., Box, J. E., van den Broeke, M. R., Miège, C., Burgess, E. W., van Angelen, J.
12 H., Lenaerts, J. T. M., Koenig, L. S., Paden, J., Lewis, C., Gogineni, S. P., Leuschen, C. and
13 McConnell, J. R.: Extensive liquid meltwater storage in firn within the Greenland ice sheet,
14 *Nat. Geosci.*, 7(2), 95–98, doi:10.1038/ngeo2043, 2013.

15 Grenfell, T. C. and Perovich, D. K.: Radiation absorption-coefficients of polycrystalline ice
16 from 400–1400 nm, *J. Geophys. Res. Atmos.*, 86(NC8), 7447–7450,
17 doi:10.1029/JC086iC08p07447, 1981.

18 Hall, D. K., Box, J. E., Casey, K. A., Hook, S. J., Shuman, C. A. and Steffen, K.: Comparison
19 of satellite-derived and in-situ observations of ice and snow surface temperatures over
20 Greenland, *Remote Sens. Environ.*, 112, 3739–3749, doi:10.1016/j.rse.2008.05.007, 2008.

21 Hall, D. K., Comiso, J. C., DiGirolamo, N. E., Shuman, C. A., Box, J. E., & Koenig, L. S.:
22 Variability in the surface temperature and melt extent of the greenland ice sheet from
23 MODIS. *Geophys. Res. Lett.*, 40(10), 2114–2120, doi: 10.1002/grl.50240, 2013.

24 Hanna, E., Fettweis, X., Mernild, S. H., Cappelen, J., Ribergaard, M. H., Shuman, C. A.,
25 Steffen, K., Wood, L. and Mote, T. L.: Atmospheric and oceanic climate forcing of the
26 exceptional Greenland ice sheet surface melt in summer 2012, *Int. J. Climatol.*, 34(4), 1022–
27 1037, doi:10.1002/joc.3743, 2014.

28 Harper, J., Humphrey, N., Pfeffer, W. T., Brown, J. and Fettweis, X.: Greenland ice-sheet
29 contribution to sea-level rise buffered by meltwater storage in firn., *Nature*, 491(7423), 240–
30 3, doi:10.1038/nature11566, 2012.

1 Hoffman, M. J., Catania, G. A., Neumann, T. A., Andrews, L. C. and Rumrill, J. A.: Links
2 between acceleration, melting, and supraglacial lake drainage of the western Greenland Ice
3 Sheet, *J. Geophys. Res. Surf.*, 116, doi:10.1029/2010JF001934, 2011.

4 Howat, I. M., de la Pena, S., van Angelen, J. H., Lenaerts, J. T. M. and van den Broeke, M.
5 R.: Expansion of meltwater lakes on the Greenland Ice Sheet, *The Cryosphere*, 7(1), 201–204,
6 doi:10.5194/tc-7-201-2013, 2013.

7 Humphrey, N. F., Harper, J. T. and Pfeffer, W. T.: Thermal tracking of meltwater retention in
8 Greenland's accumulation area, *J. Geophys. Res.*, 117(F1), F01010,
9 doi:10.1029/2011JF002083, 2012.

10 Joughin, I., Das, S. B., King, M. a, Smith, B. E., Howat, I. M. and Moon, T.: Seasonal
11 speedup along the western flank of the Greenland Ice Sheet., *Science*, 320(5877), 781–3,
12 doi:10.1126/science.1153288, 2008.

13 Khan, S. A., Kjaer, K. H., Bevis, M., Bamber, J. L., Wahr, J., Kjeldsen, K. K., Bjork, A. A.,
14 Korsgaard, N. J., Stearns, L. A., van den Broeke, M. R., Liu, L., Larsen, N.K. and Muresan, I.
15 S.: Sustained mass loss of the northeast greenland ice sheet triggered by regional
16 warming. *Nature Climate Change*, 4(4), 292-299. doi: 10.1038/nclimate2161, 2014.

17 Koenig, L. S. and Hall, D. K.: Comparison of satellite, thermochron and air temperatures at
18 Summit, Greenland, during the winter of 2008/09, *J. Glaciol.*, 56(198), 735–741, 2010.

19 Koenig, L. S., Miège, C., Forster, R. R. and Brucker, L.: Initial in situ measurements of
20 perennial meltwater storage in the Greenland firn aquifer, *Geophys. Res. Lett.*, 41(1),
21 2013GL058083, doi:10.1002/2013GL058083, 2014.

22 Kuipers Munneke, P., M. Ligtenberg, S. R., van den Broeke, M. R., van Angelen, J. H. and
23 Forster, R. R.: Explaining the presence of perennial liquid water bodies in the firn of the
24 Greenland Ice Sheet, *Geophys. Res. Lett.*, 41(2), 476–483, doi:10.1002/2013GL058389,
25 2014.

26 Lampkin, D. J.: Supraglacial lake spatial structure in western Greenland during the 2007
27 ablation season, *J. Geophys. Res.*, 116(F4), F04001, doi:10.1029/2010JF001725, 2011.

28 Lampkin, D.J., VanderBerg, J.: Supraglacial melt channel networks in the Jakobshavn Isbræ
29 region during the 2007 melt season, *Hydrol. Process.*, 28(25), doi: 10.1002/hyp.10085, 2013.

1 Langford, V. S., McKinley, A. J. and Quickenden, T. I.: Temperature dependence of the
2 visible-near-infrared absorption spectrum of liquid water, *J. Phys. Chem. A*, 105(39), 8916–
3 8921, doi:10.1021/jp010093m, 2001.

4 Leuschen, C.: IceBridge Snow Radar L1B Geolocated Radar Echo Strength Profiles, Boulder,
5 Colorado, NASA DAAC at the National Snow and Ice Data Center, accessed 2014.

6 Luck, W.A.P.: A Model of Hydrogen-Bonded Liquids, *Angewandte Chemie International*
7 *Edition in English*, 19(1), 28-41, 1980.

8 McMillan, M., Nienow, P., Shepherd, A., Benham, T. and Sole, A.: Seasonal evolution of
9 supra-glacial lakes on the Greenland Ice Sheet, *Earth Planet. Sci. Lett.*, 262(3-4), 484–492,
10 doi:10.1016/j.epsl.2007.08.002, 2007.

11 Mote, T. L.: Greenland surface melt trends 1973-2007: Evidence of a large increase in 2007,
12 *Geophys. Res. Lett.*, 34, doi:L22507 10.1029/2007gl031976, 2007.

13 Nghiem, S. V., Hall, D. K., Mote, T. L., Tedesco, M., Albert, M. R., Keegan, K., Shuman, C.
14 A., DiGirolamo, N. E. and Neumann, G.: The extreme melt across the Greenland ice sheet in
15 2012, *Geophys. Res. Lett.*, 39(20), n/a–n/a, doi:10.1029/2012GL053611, 2012.

16 Ohmura, A., Steffen, K., Blatter, H., Greuell, W., Rotach, M., Konzelmann, T., Laternser, M.,
17 Ouchi, A., Steiger, D.: Energy and mass balance during the melt season at the equilibrium line
18 altitude, Paakitsoq, Greenland ice sheet. Progress Report No. 1, Eidgenoss. Tech. Hochschule,
19 Zurich, Department of Geography, 1991.

20 Palmer, S., Shepherd, A., Nienow, P. and Joughin, I.: Seasonal speedup of the Greenland Ice
21 Sheet linked to routing of surface water, *Earth Planet. Sci. Lett.*, 302, 423–428,
22 doi:10.1016/j.epsl.2010.12.037, 2011.

23 Panzer, B., Gomez-Garcia, D., Leuschen, C., Paden, J., Rodriguez-Morales, F., Patel, A.,
24 Markus, T., Holt, B. and Gogineni, P.: An ultra-wideband, microwave radar for measuring
25 snow thickness on sea ice and mapping near-surface internal layers in polar firn, *J. Glaciol.*,
26 59(214), 244–254, doi:10.3189/2013JoG12J128, 2013.

27 Rennermalm, A. K., Smith, L. C., Chu, V. W., Box, J. E., Forster, R. R., Van den Broeke, M.
28 R., Van As, D. and Moustafa, S. E.: Evidence of meltwater retention within the Greenland ice
29 sheet, *The Cryosphere.*, 7(5), 1433–1445, doi:10.5194/tc-7-1433-2013, 2013.

1 Rodriguez-Morales, F., Gogineni, S., Leuschen, C. J., Paden, J. D., Li, J., Lewis, C. C.,
2 Panzer, B., Alvestegui, D. G.-G., Patel, A., Byers, K., Crowe, R., Player, K., Hale, R. D.,
3 Arnold, E. J., Smith, L., Gifford, C. M., Braaten, D. and Panton, C.: Advanced
4 Multifrequency Radar Instrumentation for Polar Research, *IEEE Trans. Geosci. Remote*
5 *Sens.*, 52(5), 2824–2842, doi:10.1109/TGRS.2013.2266415, 2014.

6 Selmes, N., Murray, T. and James, T. D.: Fast draining lakes on the Greenland Ice Sheet,
7 *Geophys. Res. Lett.*, 38, doi:10.1029/2011GL047872, 2011.

8 Shepherd, A., Ivins, E. R., A, G., Barletta, V. R., Bentley, M. J., Bettadpur, S., Briggs, K. H.,
9 Bromwich, D. H., Forsberg, R., Galin, N., Horwath, M., Jacobs, S., Joughin, I., King, M. A.,
10 Lenaerts, J. T. M., Li, J., Ligtenberg, S. R. M., Luckman, A., Luthcke, S. B., McMillan, M.,
11 Meister, R., Milne, G., Mouginot, J., Muir, A., Nicolas, J. P., Paden, J., Payne, A. J.,
12 Pritchard, H., Rignot, E., Rott, H., Sørensen, L. S., Scambos, T. A., Scheuchl, B., Schrama, E.
13 J. O., Smith, B., Sundal, A. V, van Angelen, J. H., van de Berg, W. J., van den Broeke, M. R.,
14 Vaughan, D. G., Velicogna, I., Wahr, J., Whitehouse, P. L., Wingham, D. J., Yi, D., Young,
15 D. and Zwally, H. J.: A reconciled estimate of ice-sheet mass balance., *Science*, 338(6111),
16 1183–9, doi:10.1126/science.1228102, 2012.

17 Sneed, W. A. and Hamilton, G. S.: Validation of a method for determining the depth of
18 glacial melt ponds using satellite imagery, *Ann. Glaciol.*, 52(59), 15–22, 2011.

19 Sundal, A. V, Shepherd, A., Nienow, P., Hanna, E., Palmer, S. and Huybrechts, P.: Evolution
20 of supra-glacial lakes across the Greenland Ice Sheet, *Remote Sens. Environ.*, 113, 2164–
21 2171, doi:10.1016/j.rse.2009.05.018, 2009.

22 Sundal, A. V., Shepherd, A., Nienow, P., Hanna, E., Palmer, S. and Huybrechts, P.: Melt-
23 induced speed-up of Greenland ice sheet offset by efficient subglacial drainage, *Nature*,
24 469(7331), 522–U83, doi:10.1038/nature09740, 2011.

25 Surdu, C. M., Duguay, C. R., Brown, L. C. and Fernandez Preto, D.: Response of ice cover on
26 shallow lakes of the North Slope of Alaska to contemporary climate conditions (1950-2011):
27 radar remote-sensing and numerical modeling data analysis, *The Cryosphere*, 8, 167-180,
28 doi:10.5194/tc-8-167-2014, 2014.

29 Tedesco M, Fettweis X, Van den Broeke M, Van de Wal R, Smeets C, Van de Berg W,
30 Serreze M, Box J.: The role of albedo and accumulation in the 2010 melting record in
31 Greenland. *Environ Res Lett* 6:014005, 2011.

1 Tedesco, M. and Steiner, N.: In-situ multispectral and bathymetric measurements over a
2 supraglacial lake in western Greenland using a remotely controlled watercraft, *The*
3 *Cryosphere*, 5(2), 445–452, doi:10.5194/tc-5-445-2011, 2011.

4 Tedstone, A. J., Nienow, P. W., Sole, A. J., Mair, D. W. F., Cowton, T. R., Bartholomew, I.
5 D. and King, M. A.: Greenland ice sheet motion insensitive to exceptional meltwater forcing,
6 *Proc. Natl. Acad. Sci. U. S. A.*, 110(49), 19719–19724, doi:10.1073/pnas.1315843110, 2013.

7 Ulaby, F.T., Moore, R. K., and Fung, A. K.: *Microwave Remote Sensing: Active and Passive.*
8 Vol. 2. Reading, Mass: Addison-Wesley Pub. Co., Advanced Book Program/World Science
9 Division, 1981.

10 Vernon, C. L., Bamber, J. L., Box, J. E., van den Broeke, M. R., Fettweis, X., Hanna, E. and
11 Huybrechts, P.: Surface mass balance model intercomparison for the Greenland ice sheet,
12 *Cryosph.*, 7(2), 599–614, doi:10.5194/tc-7-599-2013, 2013.

13 Wan, Z. M., Zhang, Y. L., Zhang, Q. C. and Li, Z. L.: Validation of the land-surface
14 temperature products retrieved from Terra Moderate Resolution Imaging Spectroradiometer
15 data, *Remote Sens. Environ.*, 83, 163–180, 2002.

16 Warren, S. G.: Optical-constants of ice from the ultraviolet to the microwave, *Appl. Opt.*,
17 23(8), 1206–1225, 1984.

18 Wiesmann, A. and Matzler, C.: Microwave emission model of layered snowpacks, *Remote*
19 *Sens. Environ.*, 70(3), 307–316, doi:10.1016/S0034-4257(99)00046-2, 1999.

20 Zwally, H. J., Abdalati, W., Herring, T., Larson, K., Saba, J. and Steffen, K.: Surface melt-
21 induced acceleration of Greenland ice-sheet flow, *Science*. 297(5579), 218–222,
22 doi:10.1126/science.1072708, 2002.

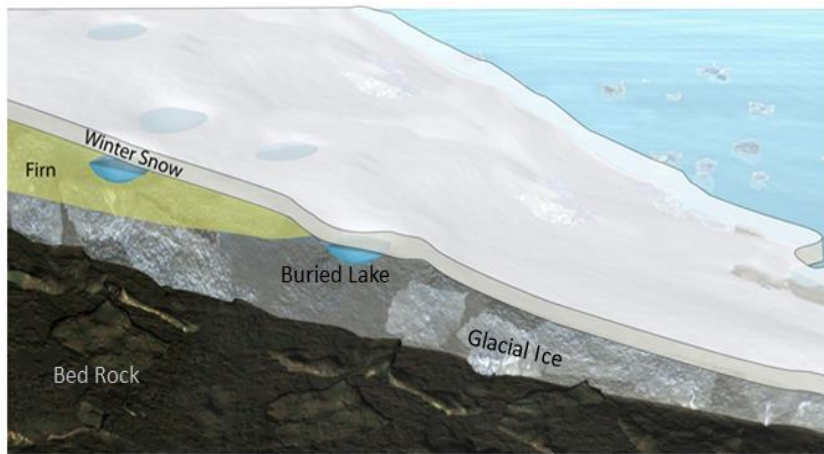
23

24 Table 1. Number of buried lakes detected in each year along with the number of lakes
25 detected per km of flightlines below 2000 m , the mean elevation and standard deviation of
26 buried lake elevations and the percentage of buried lake below 1000 m in elevation. See
27 Figure 6 for spatial distribution.

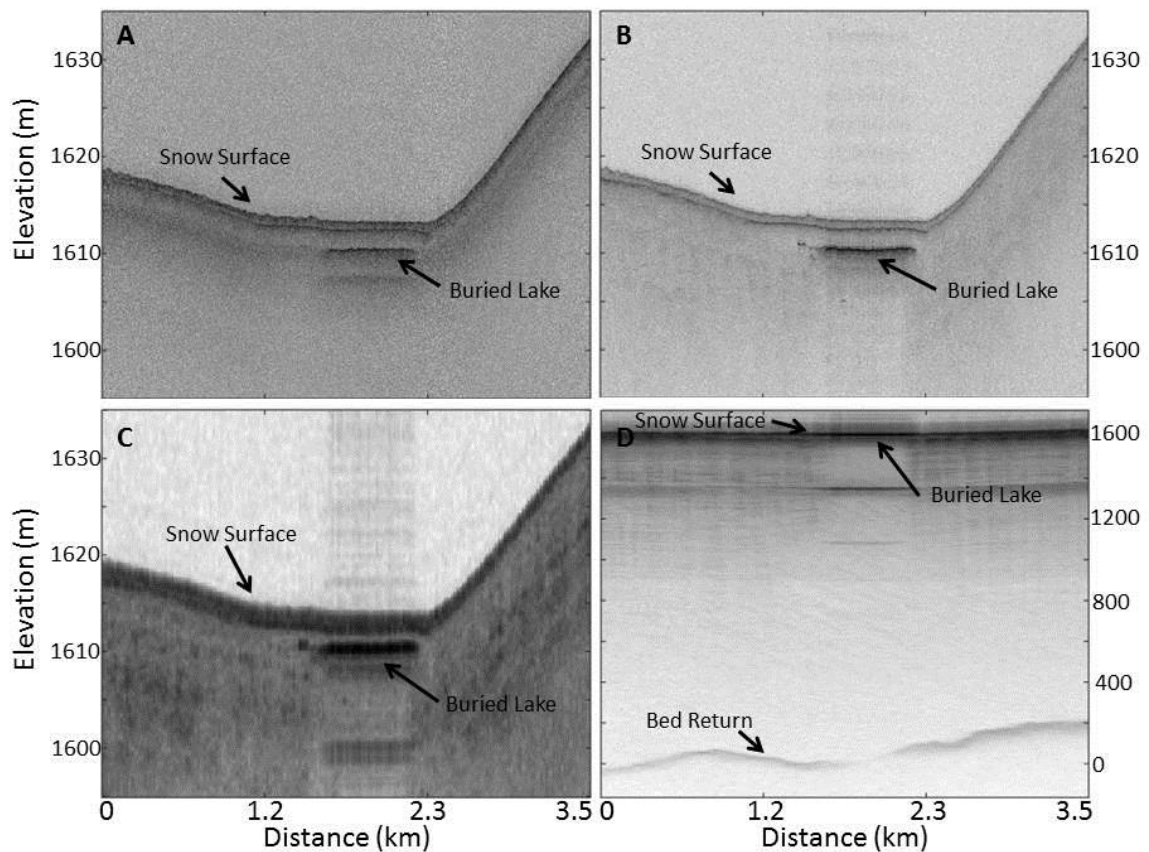
Year Collected	Buried Lakes Detected	Buried Lakes per 1000 km of flightlines	Mean Elevation (m)	Std Elevation	% of Buried Lakes Below
----------------	--------------------------	---	--------------------------	------------------	----------------------------------

		below 2000 m			1000 m
2009	57	2.1	1268	290	14
2010	85	2.2	1180	399	33
2011	174	3.9	1415	295	10
2012	127	3.1	1371	332	15

1

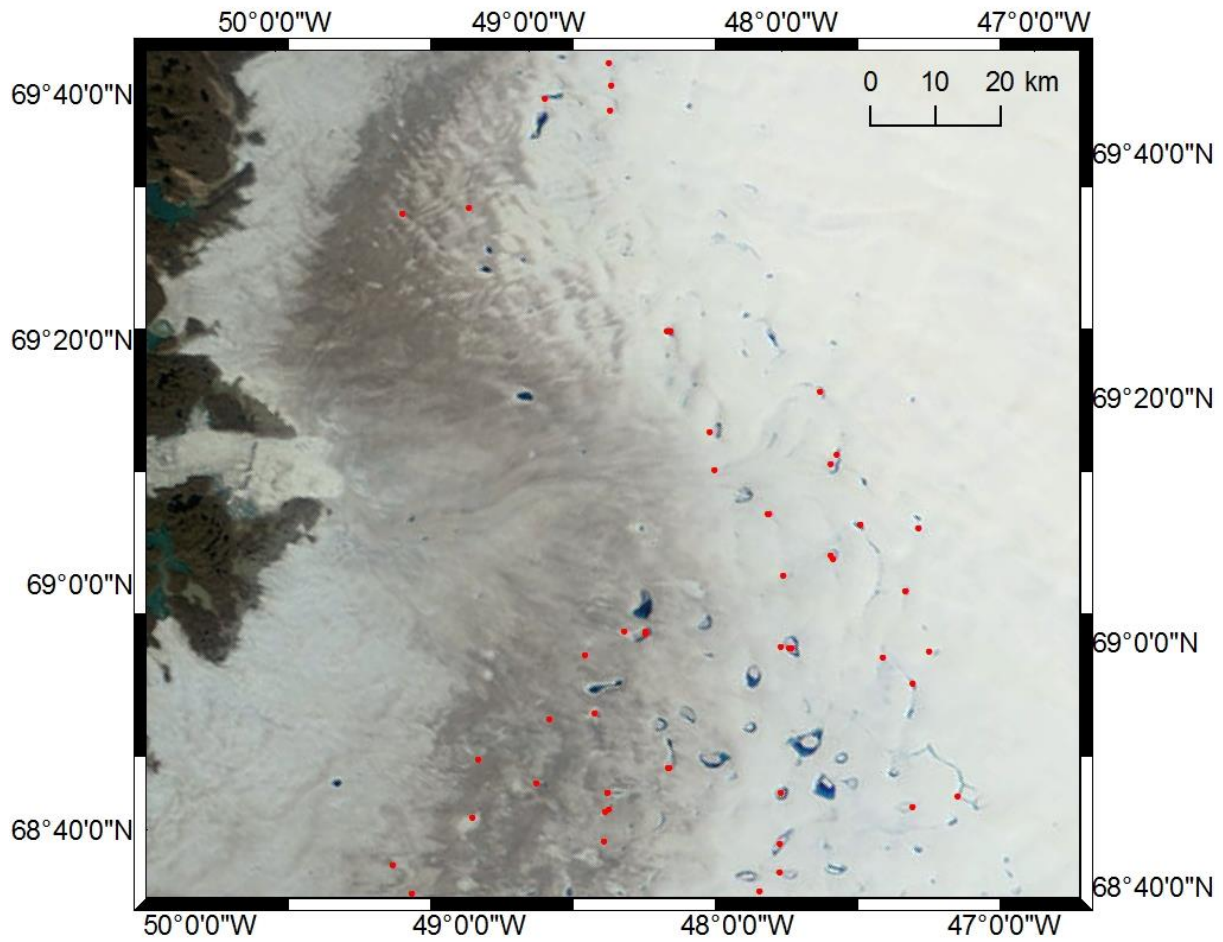


1
 2 Figure 1. An illustration showing an early spring cross sectional and perspective view of
 3 buried supraglacial lakes (blue), existing under the seasonal snow layer, still filled with water
 4 after the winter season.



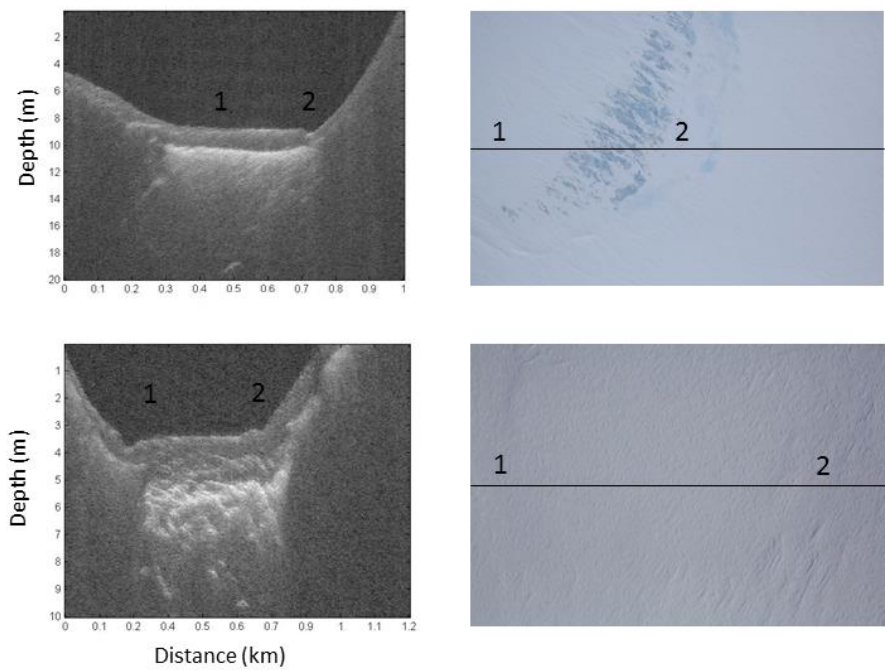
5
 6 Figure 2. Radar echograms from Western Greenland (~90 km inland of Jakobshavn's
 7 terminus) showing radar signal attenuation at multiple frequencies over a buried lake from the
 8 A) Ku-band Radar (~13-17 GHz) B) Snow Radar (~2-6.5 GHz) C) Accumulation Radar
 9 (~600-900 MHz) and D) MCoRDS Radar (~140-260 MHz).

1



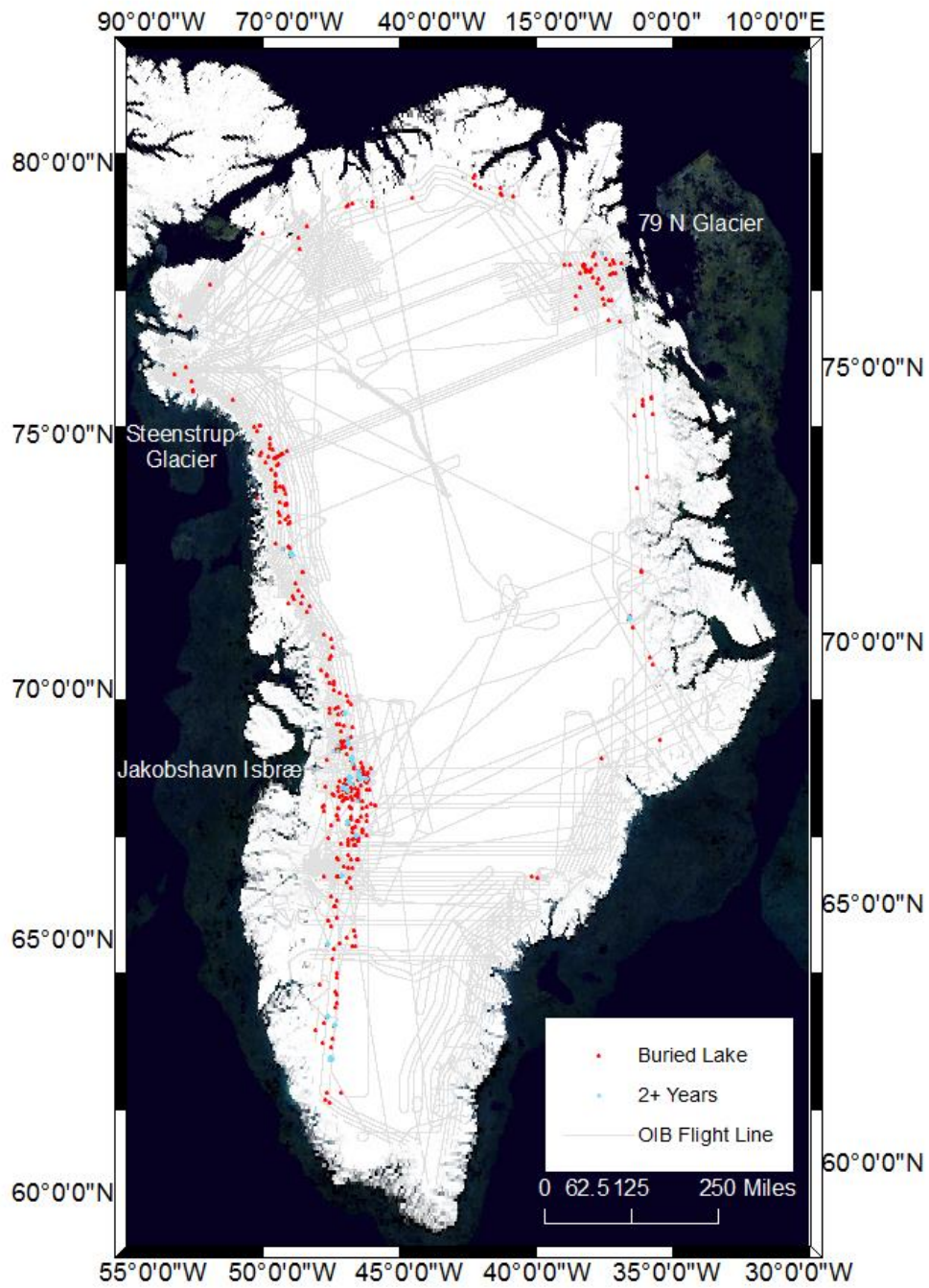
2

3 Figure 3. Radar-detected buried lake locations (red dots) overlain on MODIS Rapid Response
4 image from August 7, 2010. Note clear correspondence of radar-detected lake locations with
5 many supraglacial lakes clearly visible in this image; all the buried lakes in the dataset were
6 associated with visible supraglacial lakes captured in at least one MODIS image over the
7 analysis period.



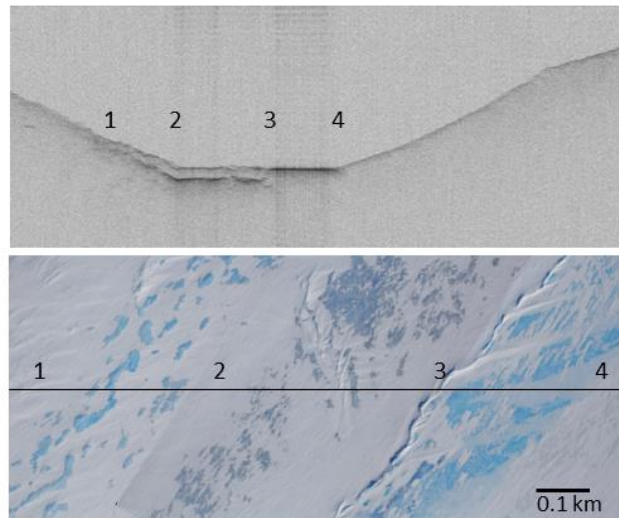
1

2 Figure 4. Snow Radar echograms of buried lakes (left) with DMS imagery of the GrIS surface
 3 (right) from: (top) a rare buried lake in Northwest Greenland (~45 km inland from the
 4 terminus of Steenstrup Glacier) with a surface expression showing darker blue where there is
 5 buried liquid water and a more turquoise, lighter blue where the lake is frozen through and
 6 (bottom) a typical buried lake in Western Greenland (~60 km inland from the terminus of
 7 Jakobshavn Isbræ) showing surface sastrugi and no detectable lake surface expression.

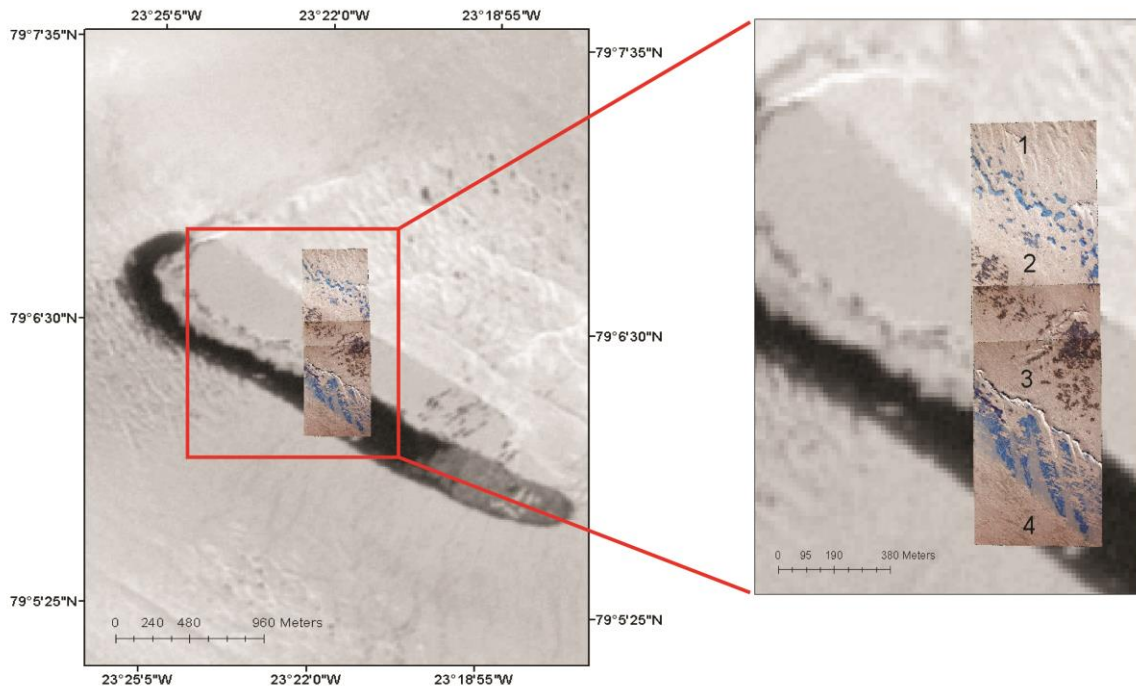


1
 2 Figure 5. Locations of buried lakes (red circles) and multi-year buried lakes (blue circles)
 3 from 2009-2012 with OIB flight lines (gray lines).

4

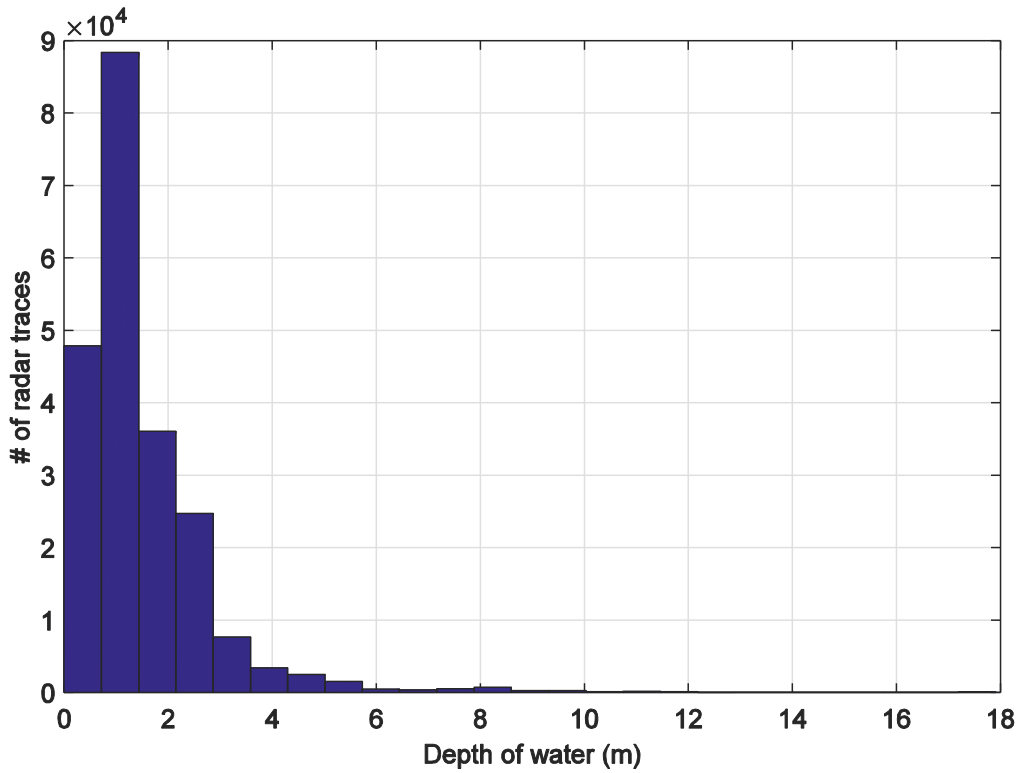


1
 2 Figure 6. Snow Radar echogram (top) with DMS image of GrIS snow surface (bottom) taken
 3 on May 2, 2011 for a buried lake in North Greenland (~100 km inland from the terminus 79 N
 4 Glacier) showing from location 1 to 2 the turquoise blue refrozen lake, from 2 to 3 the darker
 5 blue retained water, a pressure ridge at 3, and from 3 to 4 surface melt caused by radiative
 6 heating at the surface of the refrozen lake edge.



1

2 Figure 7. Image comparison of May 2, 2011 DMS image for the buried lake in Figure 6
 3 superimposed over a Landsat ETM+ image acquired on July 19, 2011, well into the melt
 4 season, when a supraglacial lake had formed. Expanded images are of the same location over
 5 the section of the lake where the early season radar data showed initial surface melt. The lake
 6 extent correlates with the early season melt area (between locations 3 and 4) and the area of
 7 stored water maintained a floating ice cap into the melt season (between locations 2 and 3).



1
 2 Figure 8. Histogram showing the depth of the water surface from every radar return over a
 3 buried lake from 2009-2012. Error estimates on the depth are on average 9% shallower due
 4 to uncertainties associated with the stratigraphy of density across the GrIS, which is used to
 5 convert radar travel time to depth.